

## NON-PERTURBATIVE DIFFRACTIVE SCATTERING \*

H.G. DOSCH

Institut für Theoretische der Physik, der Universität Heidelberg  
Heidelberg, Germany*(Received October 26, 1999)*

In the Model of the Stochastic Vacuum the infrared behaviour of QCD is approximated by a Gaussian stochastic process in the gluon field strength. This assumption leads already to confinement for non-Abelian gauge theories. The main part of the contribution is dedicated to the application of the model to soft high energy reactions as hadron-hadron scattering and electroproduction. The special role of the odderon is also investigated.

PACS numbers: 12.38.Aw, 12.38.Lg

**1. Introduction***1.1. General remarks*

To my opinion the most exciting new feature of Quantum Chromo Dynamics (QCD) as compared to quantum field theories discussed before its appearance is the phenomenon of confinement. Whereas the consequences of confinement on hadron spectroscopy have been studied extensively and have led to an at least qualitative understanding of the “particle zoo”, its implications on high energy scattering are much less obvious. The classical work of Low and Nussinov [1,2] has shown that a simple two gluon exchange is already able to reproduce qualitatively essential features of soft hadron-hadron scattering. The modification of the two gluon exchange exchange by considering non-perturbative gluon exchange related to specific properties of the QCD vacuum [3] has not only put the Low Nussinov model on a more rational basis (in the latter validity of perturbation theory was implied even for distances as large as hadron radii) but also explained a striking feature of high energy hadron-hadron scattering, namely the quark additivity rule. On the other hand the most promising scenario for confinement, the dual superconductor model of 't Hooft and Mandelstam [4,5] makes it plausible

---

\* Presented at the XXXIX Cracow School of Theoretical Physics, Zakopane, Poland, May 29–June 8, 1999.

that the gluonic string formed in hadrons plays also an important role in scattering and it has been shown that such a picture can indeed explain some systematics observed in the scattering of hadrons of different sizes [6].

The model of the stochastic vacuum [7,8] on which I shall concentrate in this approach yields confinement for non-Abelian gauge theories under very general assumptions and can be also applied to high energy scattering. It leads to a formation of a color–electric string inside hadrons and shows that this string plays an essential role in hadron–hadron scattering. Quark additivity does thus no longer hold, but it turns out that the different hadron sizes lead to the correct ratios of hadronic cross sections. Since many different approaches may lead to similar phenomenological features it is important to apply proposed models to a large variety of processes in order to obtain some insight into the basic mechanisms governing hadron–hadron scattering. In this talk I do not intend to give an exhaustive review of the subject but I shall present only the principal assumption and some results of the specific approach presented here. For more details I refer to the original literature and some specific reviews [9–11]

### 1.2. Notation

The notation I am using in the following is:  
for the color potential:

$$A_\mu^F(x) \quad \text{color } F = 1 \dots 8;$$

for the gluon field strength tensor:

$$F_{\mu\nu}^F := \partial_\mu A_\nu^F - \partial_\nu A_\mu^F + g_s f_{GHF} A_\mu^G A_\nu^H.$$

Lie-Algebra valued quantities are denoted by **bold face** symbols:

$$\mathbf{A}_\mu = \sum_C A_\mu^C \lambda_C / 2; \quad \mathbf{F}_{\mu\nu} = \sum_C F_{\mu\nu}^C \frac{\lambda_C}{2}.$$

The approach to non-perturbative QCD is based on quantization by functional integration written symbolically

$$\langle F(\psi, A) \rangle = \frac{1}{\mathcal{N}} \int \mathcal{D}\psi \mathcal{D}\bar{\psi} \mathcal{D}A F(\psi, A) e^{iS_{\text{QCD}}[\psi, \bar{\psi}, A]} \quad (1)$$

with  $S[\psi, \bar{\psi}, A] = \int d^3x dx_0 \mathcal{L}_{\text{QCD}}$ . We shall work mostly in the quenched approximation, *i.e.* no internal loops are taken into account in the integration.

1.3. Some non-perturbative results

Before I come to the more technical points let me just show shortly that a nonperturbative treatment is unavoidable in high energy scattering. If we want to calculate a dimensional quantity, *e.g.*  $\sqrt{\sigma_{pp}}$  we have:

$$\sqrt{\sigma_{pp}} = f(\alpha_s)\mu^{-1}$$

$$\frac{d\sqrt{\sigma_{pp}}}{d\mu} = 0 = f'(\alpha_s)\frac{1}{\mu}\frac{d\alpha_s}{d\mu} - \frac{1}{\mu^2}f(\alpha_s)$$

from this follows:

$$\frac{f'(\alpha_s)}{f(\alpha_s)} = \frac{1}{\beta(\alpha_s)} \tag{2}$$

with the  $\beta$ -function:

$$\mu\frac{d\alpha_s}{d\mu} = \beta(\alpha_s) = -\frac{1}{2\pi}\left(11 - \frac{2}{3}n_f\right)\alpha_s^2 + O(\alpha_s^3).$$

Integrating equation (2) yields:

$$f(\alpha_s) = f(\alpha_0)\exp\left(\int_{\alpha_0}^{\alpha_s}\frac{d\alpha'}{\beta(\alpha')}\right)$$

which cannot be expanded in a power series in  $\alpha_s$  around  $\alpha_s=0$ , because terms like  $e^{1/\alpha_s}$  occurring on the right hand side cause an essential singularity.

In scattering we use the common kinematical notation for a process  $a + b \rightarrow c + d$ :  $s = W^2 = (p_a + p_b)^2$ ;  $t = (p_a - p_c)^2$ . If particle  $a$  is a (virtual) photon, we denote its virtuality by  $Q^2 = -p_a^2$ .

We consider the following kinematical region:  $t < 1 \text{ GeV}^2$ ;  $W > 20 \text{ GeV}$ .

We shall extensively use the optical theorem relating the total cross section to the imaginary part of the elastic forward scattering:

$$\sigma_{\text{tot}} = \frac{1}{s}\text{Im}T(s, 0).$$

Axiomatic field theory leads to the Martin–Froissart bound:

$$\sigma_{\text{tot}} = O(\log^2[s]).$$

The Regge picture gives a very successful description of high energy scattering, I therefore recapitulate a few essential features.

The Regge-ansatz for the scattering amplitude is:

$$T(s, t) = \beta(t) \frac{\exp[i\pi\alpha(t)] - S}{\sin[\pi\alpha(t)]} s^{\alpha(t)}. \quad (3)$$

Regge trajectories  $\alpha(t)$  are given in the following Table

Soft (DL) pomeron:	$\alpha_P(t) = 1.08 + 0.25t/\text{GeV}^2;$	$S = 1$
Reggeon:	$\alpha_R(t) = 0.5 + t/\text{GeV}^2;$	" $S = 0$ "
Searched for:		
Odderon:	$\alpha_O(0) \approx 1$	$S = -1$
Hard pomeron:	$\alpha_{hP}(0) > 1.1$	$S = 1$

The intercepts larger than 1 cannot describe the true asymptotic behaviour since they would lead to a violation of the Froissart–Martin bound. The scattering amplitude (3) has therefore to be modified by unitarity terms at really high energies which are however beyond the present experimental limits.

## 2. High energy scattering in eikonal approximation

In soft high energy scattering there are two different scales: hard ones, the c.m. energy  $W = \sqrt{s}$  and eventually the photon virtuality  $Q^2$  and soft ones, namely the momentum transfer  $t$ , and the sizes of hadrons.

As an effect of hard energy scale  $W$  the partons move in the CM-frame on (nearly) light-like trajectories and an eikonal (semi-classical) treatment is possible.

We shall follow the treatment given by Nachtmann [12] and consider first quarks moving in an external ‘classical’ colour field and then incorporate quantization by using a non-perturbative model for the functional integration over all external field configurations denoted by  $\langle \dots \rangle_A$ .

A quark moving along a trajectory  $\Gamma$  in a color Field  $\mathbf{A}_\mu$  picks up a phase factor:  $P \exp[-ig_s \int_\Gamma \mathbf{A}_\mu dx^\mu]$

Two quarks moving on lightlike paths:  $\Gamma_\pm = (x^0, \pm \vec{b}/2, x^3 = x_0)$  receive thus the factor:

$$P \exp \left[ -ig_s \int_{\Gamma_+} \mathbf{A}_\mu dx^\mu \right] P \exp \left[ -ig_s \int_{\Gamma_-} \mathbf{A}_\mu dx^\mu \right]$$

depending on the impact parameter  $b$ .

The  $T$ -matrix element for the (fictitious) quark–quark scattering in the quenched approximation is thus given by:

$$\begin{aligned}
 T(s, t) &= i s \int d^2 b e^{i \vec{q} \cdot \vec{b}} J(\vec{b}) \\
 J(\vec{b}) &= \frac{1}{Z} \int \mathcal{D} A \exp[-i S_{YM}] P \exp \left[ -i g_s \int_{\Gamma_+} \mathbf{A}_\mu dx^\mu \right] \\
 &\quad \times P \exp \left[ -i g_s \int_{\Gamma_-} \mathbf{A}_\mu dx^\mu \right] \\
 &\equiv \left\langle P \exp \left[ -i g_s \int_{\Gamma_+} \mathbf{A}_\mu dx^\mu \right] * P \exp \left[ -i g_s \int_{\Gamma_-} \mathbf{A}_\mu dx^\mu \right] \right\rangle_A .
 \end{aligned}$$

This expression can in principle be evaluated, *e.g.* on the lattice (with gauge fixing) but the lightlike path shrinks in Euclidean metrics to (nearly) a point, so at least we have to use for the next time models in order to evaluate the integration over the external colour fields.

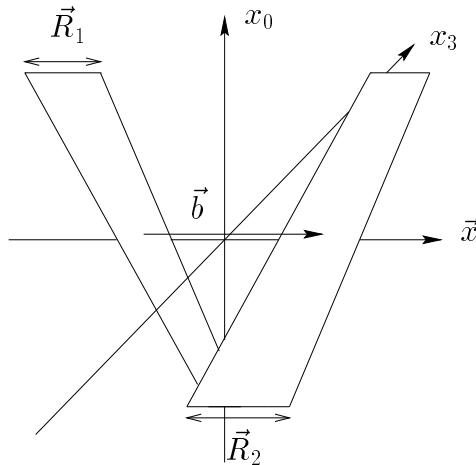


Fig. 1. Wegner–Wilson loops formed by the paths of quarks and antiquarks inside two mesons.  $\vec{R}_1$  and  $\vec{R}_2$  are the vectors in the transverse plane from the middle lines to the quark lines of meson 1 and 2 respectively. For the antiquarks the corresponding vectors are  $-\vec{R}_1$  and  $-\vec{R}_2$ . The front lines of the loops guarantee that the mesons behave as singlets under local gauge transformations.

For models it is much safer to ensure gauge invariance and indeed, in actual scattering process we have to deal with hadrons and not with quarks and therefore near each quark there is an antiquark moving on a (nearly) lightlike trajectory too and we have in the femtouniverse the picture depicted in Fig. 1 which may serve as a building block for hadron–hadron scattering [13, 14].

A quark antiquark pair in a color singlet state moving in a color field  $\mathbf{A}_\mu$  on parallel lightlike lines picks thus up as phase factor a trace of Wegner–Wilson-loop:

$$W_+ = \text{tr} \left( \frac{1}{N_C} P \exp \left[ -ig_s \oint_{S_+} \mathbf{A}_\mu dx^\mu \right] \right)$$

which depends on the transversal extension  $\vec{R}$  of the loop.

The  $T$ -matrix element for dipole–dipole scattering (quenched) reads:

$$T(s, t, \vec{R}_+, \vec{R}_-, z_+, z_-) = is \int d^2b e^{i\vec{q}\vec{b}} J(\vec{b}, \vec{R}_+, \vec{R}_-, z_+, z_-),$$

$$J(\vec{b}, \vec{R}_+, \vec{R}_-, z_+, z_-) = \langle W_+ W_- \rangle_A \quad |\vec{q}|^2 = -t.$$

For consistency the impact parameter  $b$  has to be the distance of the lightcone barycenter of the partons [15] (see figure 2), the profile function  $J$  depends therefore (weakly) on the longitudinal momentum fraction  $z$  of the partons.

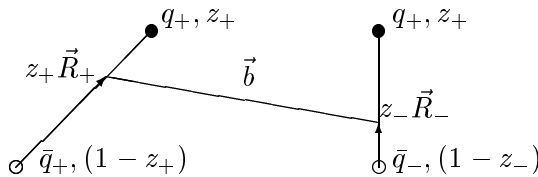


Fig. 2. The definition of the impact parameter.  $z_\pm$  is the fraction of longitudinal momentum carried by the quark on the path  $\Gamma_\pm$ .

A hadronic scattering process  $h_1 + h_2 \rightarrow h_3 + h_4$  is given by:

$$T(s, t) = \int dz_+ dz_- d^2R_+ d^2R_- T(s, t, \vec{R}_+, \vec{R}_-, z_+, z_-)$$

$$\times \psi_1(\vec{R}_+, z_+) \psi_2(\vec{R}_-, z_-) \psi_3^*(\vec{R}_+, z_+) \psi_4^*(\vec{R}_-, z_-), \quad (4)$$

where  $\psi_h(\vec{R}_+, z_+)$  is a transverse (light cone) wave function depending on the transverse coordinates  $\vec{R}$  and the longitudinal momentum fraction  $z$ .

We have to construct a model for the scattering of dipoles, where the dipoles may be large and hence the scattering process has to be treated nonperturbatively. This is in contradistinction to quarkonium–quarkonium scattering where the dipoles are assumed to be small and hence the scattering can be treated perturbatively, but the distribution function is non-perturbative, see *e.g.* [16, 17].

In order to arrive at the scattering amplitudes for baryons [14], we have to construct the analogs of the traces of the loops  $W$  in the way depicted in figure 3

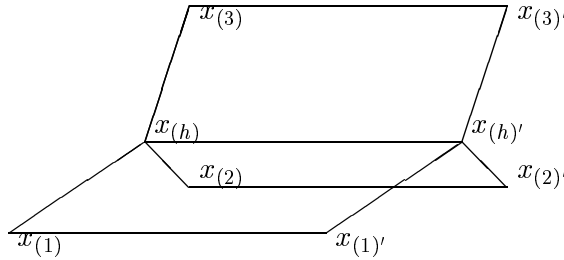


Fig. 3. The path of a baryon constructed from quark paths

The analogue of the dipole as starting point for a meson is the following expression

$$\epsilon_{abc}\epsilon_{a'b'c'}(\Gamma_{+1})_{a,a'}(\Gamma_{+2})_{b,b'}(\Gamma_{+3})_{c,c'} \tag{5}$$

with

$$\Gamma_i = \Phi(x_{(h)}, x_{(i)})\Phi(x_{(1)}, x_{(i)'})\Phi(x_{(i)'}, x_{(h)'})$$

and

$$\Phi(\Gamma)_{ab} = \left( P \int \exp \left[ -ig_s \int_{\Gamma} \mathbf{A}_{\mu} dx^{\mu} \right] \right)_{ab} .$$

Since in SU(3) we have:  $\epsilon_{abc}\Phi_{a,a'}\Phi_{b,b'}\Phi_{c,c'} = \epsilon_{a'b'c'}$  we can express Eq. (5) through Wegner–Wilson loops (without traces):

$$\epsilon_{abc}\epsilon_{a'b'c'}(\Gamma_{+1})_{a,a'}(\Gamma_{+2})_{b,b'}(\Gamma_{+3})_{c,c'} = \epsilon_{abc}\epsilon_{a'b'c'}(W_{+1})_{a,a'}(W_{+2})_{b,b'}(W_{+3})_{c,c'}$$

with

$$(W_{+i})_{a,a'} = (\Phi(x_{(h)}, x_{(i)})\Phi(x_{(i)}, x_{(i)'})\Phi(x_{(i)'}, x_{(h)})\Phi(x_{(h)'}, x_{(h)}))_{a,a'} . \tag{6}$$

For practical — and also for phenomenological — reasons we shall work often in the diquark picture, where the distance between two quarks is zero (small).

Since two quarks coupled antisymmetrically  $q_a q_b \epsilon_{abc}$  transform in  $SU(3)$  like an antiquark  $\bar{q}_c$  the baryon in the diquark picture can be treated like a meson.

### 3. Model of the stochastic vacuum (MSV)

The model of the stochastic vacuum (MSV) [7, 8] (for reviews see [9–11, 18, 19]) is the underlying model for non-perturbative QCD used in the following for calculating soft high energy scattering. I shall only sketch roughly the principal ideas and consequences of the model and refer to the original literature and reviews for more details. The basic assumption of the model is that the infrared behaviour of QCD can be **approximated** by a **Gaussian** stochastic process in the gluon **field strength**.

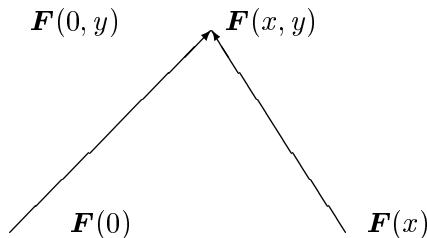
Formally this can be written as:

$$\int_{|k| < \mu} \mathcal{D}A_\rho^C e^{S_{YM}} \approx \int \mathcal{D}F_{\mu\nu}^C \exp\left(-g_s^2 \int dx dy F_{\mu\nu}^F(x) K^{-1}_{\mu\nu\kappa\lambda}{}^{FG}(x, y) F_{\kappa\lambda}^G(y)\right). \quad (7)$$

So the full domain of nonperturbative QCD is governed by the single correlator  $K_{\mu\nu\kappa\lambda}{}^{FG}$ .

In order to make the non-local correlator gauge invariant we have parallel transported all color fields to a reference point  $y$ :

$$\mathbf{F}_{\mu\nu}(x, y) = \phi(x, y) \mathbf{F}_{\mu\nu}(x) \phi(y, x) \quad (8)$$



If we neglect the dependence on the reference point  $y$  the most general form for the correlator  $K_{\mu\nu\kappa\lambda}{}^{FG}$  contains two independent scalar functions,  $D$  and  $D_1$ .

$$\begin{aligned}
 K_{\mu\nu\kappa\lambda}^{FG}(x, y) &= \langle g_s^2 F_{\mu\nu}^F(x, y) F_{\kappa\lambda}^G(0, y) \rangle = \frac{\delta^{FG} \langle g_s^2 FF \rangle}{12(N_c^2 - 1)} \\
 &\times \{ (\delta_{\mu\kappa} \delta_{\nu\lambda} - \delta_{\mu\lambda} \delta_{\nu\kappa}) D(x^2) \kappa \\
 &+ \left[ \frac{1}{2} \frac{\partial}{\partial x_\mu} (x_\kappa \delta_{\nu\lambda} - x_\lambda \delta_{\nu\kappa}) + \frac{1}{2} \frac{\partial}{\partial x_\nu} (x_\lambda \delta_{\mu\kappa} - x_\kappa \delta_{\mu\lambda}) \right] \\
 &\times D_1(x^2) (1 - \kappa) \} . \tag{9}
 \end{aligned}$$

In an Abelian gauge theory without monopoles, like QED, the homogeneous Maxwell equations imply:  $\kappa = 0$ , *i.e.* only the term with  $D_1$  can contribute.

Gaussian factorization implies:

$$\begin{aligned}
 \langle F^A F^B F^C F^D \rangle &= \langle F^A F^B \rangle \langle F^C F^D \rangle \\
 &+ \langle F^A F^C \rangle \langle F^B F^D \rangle + \langle F^A F^D \rangle \langle F^B F^C \rangle . \tag{10}
 \end{aligned}$$

The model is therefore characterized by essentially two parameters: The value of the correlator at zero distance (the gluon condensate [20]) and the correlation length.

Under this assumption we can evaluate the Euclidean Wegner–Wilson loop of width  $r$  and length  $x_4$  using the non-Abelian Stokes theorem [21–23]:

$$\left\langle P \exp \left[ -ig_s \oint \mathbf{A}_\mu dx^\mu \right] \right\rangle_A = \left\langle P \exp \left[ -ig_s \int \mathbf{F}_{\mu\nu} d\sigma^{\mu\nu} \right] \right\rangle . \tag{11}$$

The static potential is then obtained as:

$$V(r) = \lim_{x_4 \rightarrow 0} \frac{-1}{x_4} \log \left[ \left\langle P \exp \left[ -ig_s \int \mathbf{F}_{\mu\nu} d\sigma^{\mu\nu} \right] \right\rangle \right] .$$

Inserting (9) and (10) we obtain linear confinement for non-Abelian gauge theories:

$$V(r) \rightarrow r \frac{\pi\kappa}{24N_C} \langle g_s^2 FF \rangle \int dx^2 D(x^2) . \tag{12}$$

Since only the term proportional to  $D$  contributes, an Abelian gauge theory without monopoles cannot lead to confinement and a non-Abelian one leads to confinement only if  $\kappa \neq 0$ . Lattice calculations [24, 25] have shown that this typical non-Abelian term is indeed dominant in QCD, since  $\kappa \approx 0.8$ .

The model yields also the correct spin structure of potentials between heavy quarks [26–28].

Let me emphasize that an Abelian gauge theory with magnetic monopoles can have  $\kappa \neq 0$  and hence leads to confinement. Furthermore, the assumption of a Gaussian process is necessary for direct applications, but the convergence of cluster expansion alone is already enough in order to yield linear confinement [7].

The physical reason for confinement can also be investigated in the model. One can calculate the gauge invariant color field energy density produced by a static quark–antiquark pair and obtains that a color electric flux tube is formed. The results of the calculations with the model of the stochastic vacuum [29] show qualitative agreement with numerical calculations on the lattice [30] (in SU(2)-gauge theory):

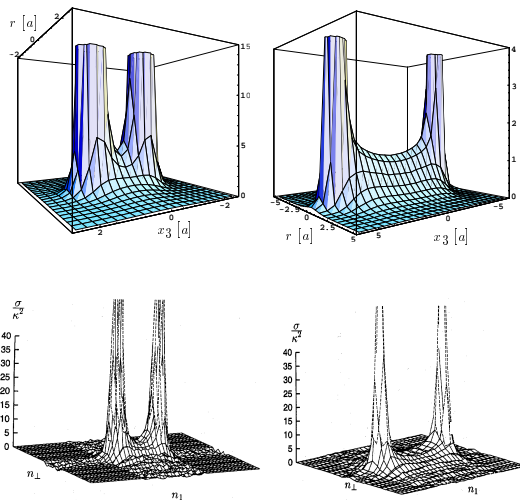


Fig. 4. The energy density of the colour fields induced by a static quark antiquark pair as calculated in the MSV (top) [29] and on the lattice (bottom) [30]

## 4. Application of the MSV to high energy scattering

### 4.1. Formalism and general results

We now use the MSV as described in Section 3 in order to calculate the dipole–dipole scattering amplitude derived in the eikonal approach in Section 2. The basic formalism of this section has been developed in [13, 14], the application to high energy processes involving (virtual) photons in [15, 31]; energy dependence has been incorporated in [32].

The starting point is equation (3):

$$J(\vec{b}, \vec{R}_+, \vec{R}_-, z_+, z_-) = \langle W_+ W_- \rangle_A \quad (13)$$

with the basic input:

$$W_+ = \text{tr} \left( \frac{1}{N_C} P \exp \left[ -ig_s \oint_{S_+} \mathbf{A}_\mu dx^\mu \right] \right).$$

As in Section 3, equation (11) we use the non-Abelian Stokes Theorem:

$$W_+ = \text{tr} \left( \frac{1}{N_C} P \exp \left[ -ig_s \int_{\Sigma_+} \mathbf{F}_{\mu\nu} d\sigma^{\mu\nu} \right] \right) \tag{14}$$

and Gaussian factorization (10) in order to evaluate the expectation value of two Wegner–Wilson loops:

$$\left\langle \text{tr} \left( \frac{1}{N_C} P \exp \left[ -ig_s \int_{\Sigma_+} \mathbf{F}_{\mu\nu} d\sigma^{\mu\nu} \right] \right) \times \text{tr} \left( \frac{1}{N_C} P \exp \left[ -ig_s \int_{\Sigma_-} \mathbf{F}_{\mu\nu} d\sigma^{\mu\nu} \right] \right) \right\rangle_A.$$

In a straightforward method [13, 14] the exponentials in this equation can be expanded in power series of the field strength tensor and Gaussian approximation can be used for the resulting products. In a more sophisticated approach [33] one can use the cumulant expansion for the product group  $SU(3) \otimes SU(3)$ . For small momentum transfer both methods give similar results, for values of  $t \approx 0.5 \text{ GeV}^2$  the second method is certainly more appropriate, since it guarantees local unitarity even for small impact parameters. The reference point  $y$  introduced in (8) must be common to both surfaces  $\Sigma_+$  and  $\Sigma_-$ .

A ‘reasonable’ choice of the surfaces obtained after applying the non-Abelian Stokes theorem has little effect on the results and can generally be absorbed in a slightly different choice of the parameters. The standard choice for the surfaces in all phenomenological applications is given in figure 5.

The expression obtained in this way contains  $I = 0$  and both  $C, P = \pm 1$  exchange, *i.e.* in Regge terminology the pomeron and the odderon exchange.

The lowest contribution, *i.e.* the quadratic term from each exponential corresponds to the  $C = P = +1$  exchange, *i.e.* the pomeron, the cubic terms to  $C = P = \pm 1$  exchange, *i.e.* the odderon. We come back to the odderon problem later.

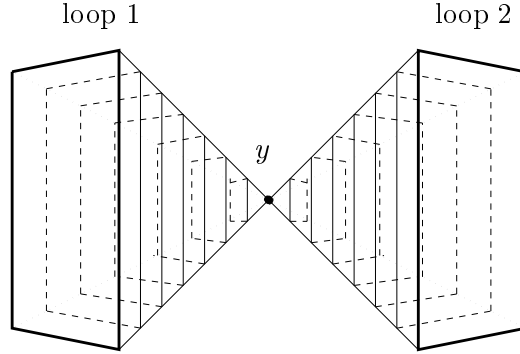


Fig. 5. Somewhat tilted view of the loops after applying the non-Abelian Stoke's theorem with the reference point  $y$  which is common to both surfaces.

There is however a fundamental problem:

The MSV as approximation to a stochastic process is primarily manageable in Euclidean field theory (like lattice gauge theory). But for high energy scattering processes the Euclidean description is very delicate, since the lightlike paths introduced above shrink to points in Euclidean field theory. We can however introduce an Minkowski version of the MSV in momentum space and at the end it turns out that only the Euclidean part of the correlators matter, *i.e.* we can safely use the Euclidean input.

This is done in the following way:

- (1) We first express correlators through Fourier transforms:

$$\begin{aligned}
 \langle g^2 F_{\mu\nu}^C(x, y) F_{\rho\sigma}^D(y, y) \rangle_B &= \frac{\delta^{CD}}{N_c^2 - 1} \frac{1}{12} \langle g^2 GG \rangle \\
 &\times \int \frac{d^4 k}{(2\pi)^4} e^{-ik(x-z)/a} \left\{ (g_{\mu\rho}g_{\nu\sigma} - g_{\mu\sigma}g_{\nu\rho}) \kappa i \tilde{D}_M(k^2) \right. \\
 &\left. + (-g_{\nu\sigma}k_\mu k_\rho + g_{\nu\rho}k_\mu k_\sigma - g_{\mu\rho}k_\nu k_\sigma + g_{\mu\sigma}k_\nu k_\rho)(1 - \kappa) i \frac{d\tilde{D}_{1M}(k^2)}{dk^2} \right\}.
 \end{aligned}
 \tag{15}$$

- (2) We then evaluate the surface integral over the sliding sides of the pyramids as volume integrals minus the surface integral over the basis using Gauss theorem.

(3) We realize that we have integrals over lightlike paths like the one

$$\lim_{T \rightarrow \infty} \lim_{L \rightarrow \infty} \int_{-T}^T dx^0 \int_{-L}^L dx^3 \delta(x^3 - x^0) \dots \tag{16}$$

from pyramid ‘+’ and a corresponding expression from ‘-’. Together with the exponentials from the Fourier transform in (15) this gives rise to the integral:

$$\begin{aligned} &\lim_{T \rightarrow \infty} \dots \lim_{L \rightarrow \infty} \int_{-T}^T dx^0 dx^3 dy^0 dy^3 \delta(x^3 - x^0) \delta(y^3 + y^0) \\ &\times \exp i \left[ k^0 (x^0 - y^0) - k^3 (x^3 + y^3) \right] \dots \dots \end{aligned} \tag{17}$$

Such an integral yields a factor

$$(2\pi)^2 \delta(k_0 - k_3) \delta(k_0 + k_3)$$

and hence the correlator  $\tilde{D}_M(k^2)$  is evaluated only at  $k_0 = 0$  *i.e.* in the Euclidean region. The correlators depending on the Euclidean momenta  $\vec{k}_T$  are obtained as two dimensional Fourier transforms of the Euclidean correlators introduced in Section 3.

Before we come to detailed applications I want to quote some **general results**:

- (1) The model introduces no new energy dependence, *i.e.* the scattering amplitudes  $T$  are proportional to  $s$  and the cross sections are therefore energy independent.
- (2) The invariants  $D$  and  $D_1$  of the correlator (9) lead to completely different behaviour of the cross section  $\sigma$  with the dipole size  $R$ :  $D$ , the Abelian, nonconfining structure leads to  $\sigma \propto \text{const}$  whereas  $D_1$ , the non-Abelian, confining structure: implies a cross section which rises with the dipole size  $R$ , see figure 6.

A further investigation shows [14], that the rise of the cross section with dipole size is due to an interaction of the strings described in Section 3, figure 4. Hence the same mechanism which leads to string formation and confinement also leads to string-string interaction in scattering.

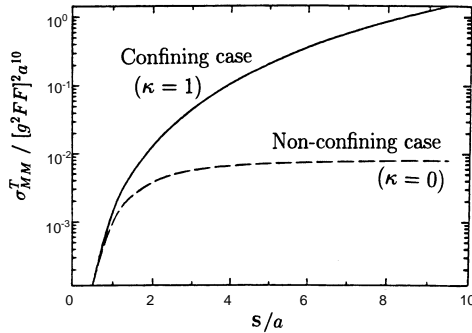


Fig. 6. The dependence of the total dipole–dipole cross section on the size of the dipoles for the Abelian correlator  $D_1$  and the confining correlator  $D$ .

#### 4.2. Parameters of the model and hadron–hadron scattering

In order to make specific predictions for various high energy reactions we have to fix the parameters of the model. They are for the MSV itself:

- (1) the correlation length;
- (2) the correlator at zero distance (Gluon condensate [20]);
- (3) the form of the correlation functions;

and for the hadrons:

- (4) the transversal wave function of the scattered hadrons;

and finally there is for hadrons a weak dependence on:

- (5) the longitudinal momentum fraction.

The parameters of the fundamental correlator (9) are constrained by:

- (1) the string tension, see equation (12);
- (2) QCD sum rules [20] (the gluon condensate) and finally we have as most important source of information;
- (3) lattice calculations [24, 25, 34].

For the second group of parameters we have the following constraints:

- Electromagnetic form factors of hadrons; decay constants of mesons; and we get some important hints from quark hadron duality and from the non-relativistic quark model.
- For photons with high virtuality we may use perturbative QCD.

These constraints allow us to estimate the parameters and therefore to predict the dipole–dipole cross sections without using any information from high energy scattering. Using for the correlation length  $a \approx 0.35$  fm, the gluon condensate  $\langle g_s^2 FF \rangle \approx 3 \text{ GeV}^4$ <sup>1</sup>. The transverse radius of proton is estimated from the electromagnetic form factor to  $\approx 0.8$  fm.

In reference [36] the dipole–proton cross sections were reconstructed from the photoproduction data. The results of this analysis are displayed as points with error bars in figure 7. The solid line shows the prediction of the MSV [37] with the parameters given above. The qualitative agreement shows that it is indeed possible to calculate high energy cross sections from low energy data.

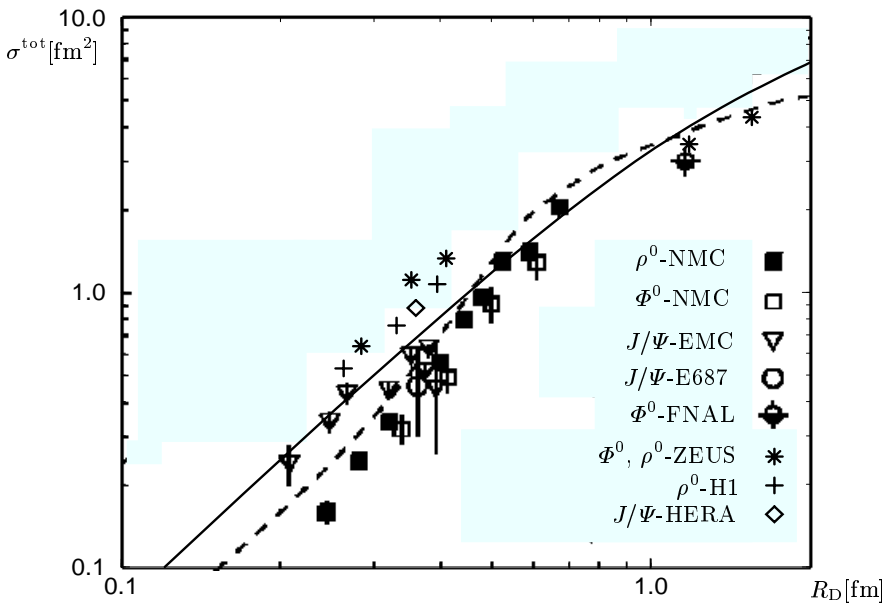


Fig. 7. Comparison of our result for the total cross section for dipole (extension  $R_D$ ) proton scattering with values extracted from cross sections of lepto-production of vector–mesons by the method of Nemchik *et al.* [36]. The solid line is our result [37] without any fitting of the parameters to high-energy data. The dashed line is the ansatz of Nemchik *et al.* for the total cross section.

In order to determine the parameters more precisely we make use of experimental input from proton–proton scattering and adjust the form of the correlators to the results of the lattice calculations. A convenient form

<sup>1</sup> In a quenched theory in which we are working the gluon condensate is expected to be about a factor 3 larger than in the case of full QCD, see [35]

of the input correlators which allows an analytic continuation and which gives a perfect agreement with the lattice data [34] is:

$$D\left(\frac{z^2}{a^2}\right) = \int \frac{d^4k}{(2\pi)^4} e^{ikz/a} \tilde{D}(k^2) \quad \tilde{D}(k^2) = \frac{27\pi^4}{4\left(k^2 - \frac{9\pi^2}{64}\right)^4}. \quad (18)$$

For the determination of the parameters we also use data from proton–(anti)proton scattering at  $s = 20$  GeV and arrive to the following values:  $a = 0.346$  fm,  $\langle g^2 FF \rangle = 2.49$  GeV,  $\kappa = 0.74$ ,  $S_p = 0.739$  fm.

#### 4.3. Results for hadron–hadron scattering

Once the parameters are fixed, we can calculate all possible hadron–hadron cross sections once we know the transversal extension. For the  $\pi$  and  $K$ -meson we assume that the transverse extension is proportional to the electromagnetic radius. For the  $J/\Psi$  we use the experimental electromagnetic width. Results of the model are displayed in Table I.

TABLE I

Ratios of different total hadronic cross sections to the proton–proton cross section at  $W = 20$  GeV.

Quantity	Model	Reference	Experiment
$\sigma_{\pi p}/\sigma_{pp}$	0.66	[14]	0.63
$\sigma_{Kp}/\sigma_{\pi p}$	0.82	[14]	0.87
$\sigma_{J/\Psi}/\sigma_{pp}$	0.12	[38]	-
$\sigma_{\Psi'}/\sigma_{pp}$	0.49	[38]	-
$B_{pp} - B_{\pi p}$	1.30	[14]	2.48
$B_{\pi p} - B_{Kp}$	0.4	[14]	0.3

It should be remarked that the correct ratio  $\sigma_{\pi p}/\sigma_{pp} \approx 2/3$  is in the model not a consequence of quark additivity, but due to the different (measured) electromagnetic radii.

#### 4.4. Reactions involving photons (real and virtual)

For high energies the dominant contribution to photon hadron interactions in the CM or hadron rest frame is the splitting of the photon into a quark antiquark pair and the subsequent interaction of the quark–antiquark pair with the hadron. We can therefore use the general equation (4) also in order to calculate high energy interactions involving photons by choosing for the corresponding transverse wave function the light cone wave function of the photon. The kinematical and internal variables are defined in figure 8.

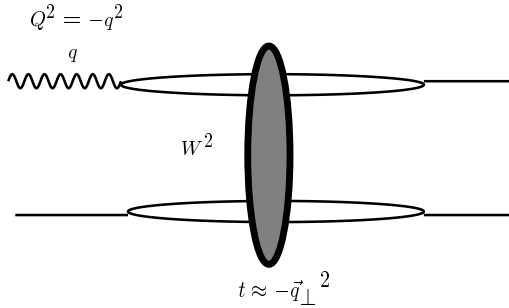


Fig. 8. Sketch of the dynamical and light cone variables entering the photonproduction off hadrons: Transverse momentum  $\vec{k}_\perp$  resp. extension  $\vec{R}_\perp$ ; longitudinal momentum fraction  $z$ ; virtuality of photon:  $Q^2 = -q^2$ , total Energy:  $s = W^2$ , momentum transfer  $\vec{q}$ .

Whereas the photon wave function at high virtualities  $Q^2$  can be calculated by perturbation theory, this is not the case for low virtualities. Usually vector meson dominance is applied, but we shall show that quark hadron duality allows a more economical description of the photon wave function at low virtualities, which interpolates smoothly to high virtualities and even takes care of the “hard part of the photon” at low virtualities. This is especially relevant for photon–photon interactions.

Let us begin with a model investigation with scalar photons and quarks as given in [31]. In such a case the “photon”-wave function at high virtualities would be given by:

$$\begin{aligned} \tilde{\psi}_\gamma(\vec{k}_\perp) &= \frac{1}{\vec{k}_\perp^2 + z(1-z)Q^2 + m_f^2}, \\ \psi_\gamma(\vec{R}_\perp) &= \frac{1}{2\pi} K_0(\sqrt{z(1-z)Q^2 + m_f^2} |\vec{R}_\perp|). \end{aligned} \tag{19}$$

For low  $Q^2$  however we expect confinement to modify these perturbative expressions considerably.

Indeed the structure of (19) is the same as that of a free nonrelativistic Greens function:

$$G_0(\vec{R}_\perp, 0, M) = \frac{m}{\pi} K_0(\sqrt{2mM} |\vec{R}_\perp|), \tag{20}$$

where  $M = -E$  stands for the virtuality  $Q^2$ .

As as been pointed out in reference [20] the harmonic oscillator is a very reasonable model for QCD: it shows both confinement and asymptotic

freedom. We therefore investigate the effects of confinement by comparing the free Green's function (20) with that of the full harmonic oscillator which can be calculated easily.

$$G_H(\vec{R}_\perp, 0, M) = \sum_{n_1, n_2} \frac{\psi_{\vec{n}}(\vec{R}_\perp) \psi_{\vec{n}}(\vec{R}_\perp)}{(n_1 + n_2 + 1)\omega + M}. \quad (21)$$

As can be seen from figures 9 Green's functions with the shift:  $M \rightarrow M + s(M)$  yield an excellent fit to the exact Green's functions. Vector dominance corresponds to keeping one or a few terms in the sum of equation (21) which leads visibly to a poorer fit to the wave function.

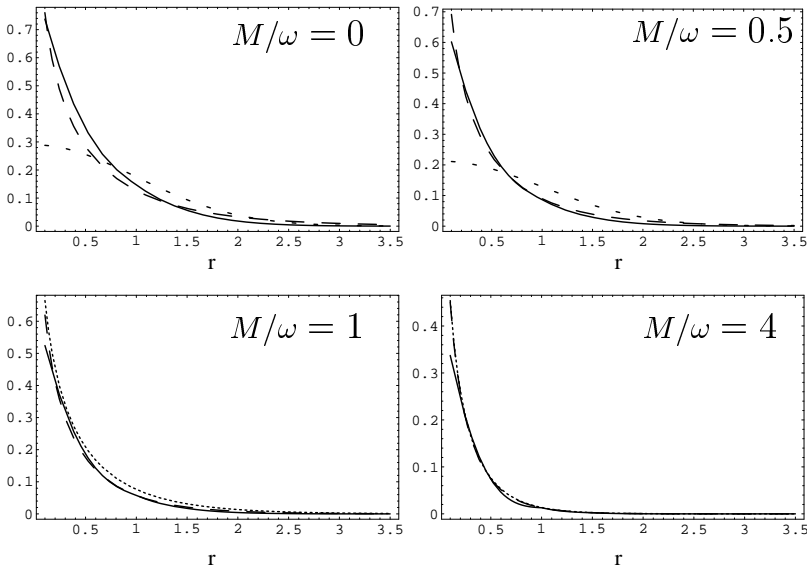


Fig. 9. Green functions (in units of  $m$ ) of an harmonic oscillator as function of  $r$  (in units of  $1/\sqrt{\omega m}$ ) for different values of  $M/\omega$ . Solid line: exact Green function  $G(r, 0, M)$ , long dashes: our approximation  $G_a(r, 0, M, s_0)$ , *i.e.*, the shifted free Green function; short dashes: approximation with two resonances, corresponding to generalized vector dominance; dots: free Green function.

We transfer this procedure to QCD by performing a  $Q^2$  dependent shift of the flavor mass  $m_f \rightarrow m_f + m(Q^2)$  in the perturbative photon wave function. The shift  $m(Q^2)$  can be fixed by a fit to the phenomenologically known vector-current twopoint function and thus introduces no new parameter. The following linear parametrizations can be used [31]:

$$\begin{aligned} m_{\text{eff}}(Q^2) &= 0.22 (1.0 - Q^2/Q_0^2), \text{ in GeV, for } Q^2 \leq Q_0^2 = 1.05 \text{ GeV}^2, \\ m_{\text{eff}}(Q^2) &= 0, \text{ for } Q^2 \geq Q_0^2. \end{aligned} \quad (22)$$

$$\begin{aligned}
 m_{s\text{eff}}(Q^2) &= 0.15 + 0.16 (1.0 - Q^2/Q_0^2), \text{ in GeV, for } Q^2 \leq Q_0^2 = 1.6 \text{ GeV}^2, \\
 m_{s\text{eff}}(Q^2) &= 0.15, \text{ for } Q^2 \geq Q_0^2.
 \end{aligned}
 \tag{23}$$

We see that above  $Q^2 = 1.05$  resp.  $1.6 \text{ GeV}^2$  the perturbative expression with the Lagrangian quark mass is used.

The resulting wave functions for the longitudinal and transverse photon are:

$$\begin{aligned}
 \psi_{\gamma,0} &= -\frac{e_f}{2\pi} \sqrt{N_c} \delta_{f\bar{f}} \delta_{h,-\bar{h}} 2z(1-z) Q K_0(\sqrt{z(1-z)Q^2 + m^2(Q^2)} |\vec{R}_\perp|), \\
 \psi_{\gamma,1} &= -\frac{e_f}{2\pi} \sqrt{2N_c} \delta_{f\bar{f}} \{i e^{i\theta} (z\delta_{h_+}\delta_{\bar{h}_-} - (1-z)z\delta_{h_-}\delta_{\bar{h}_+}) \\
 &\quad \times \sqrt{z(1-z)Q^2 + m^2(Q^2)} K_1(\sqrt{z(1-z)Q^2 + m^2(Q^2)} |\vec{R}_\perp|) \\
 &\quad + m(Q^2)\delta_{h_+}\delta_{\bar{h}_+} K_0(\sqrt{z(1-z)Q^2 + m^2(Q^2)} |\vec{R}_\perp|)\}.
 \end{aligned}
 \tag{24}$$

The longitudinal wave function has a factor  $Q$  as compared to the transverse wave function and vector meson production dominates at large  $Q^2$  but one should note that the ‘‘hadronic size’’ of the virtual photon is determined by  $1/\sqrt{z(1-z)Q^2}$  and that the transverse photon has no suppression at  $z = 0$ , and 1; hence a transverse photon can be large (*i.e.* non-perturbative) even at fairly large values of  $Q^2$ .

We have calculated in the model [15,31,39] the following reactions and compared to experiment (at  $W = 20 \text{ GeV}$ ):

$$\gamma^{(*)}p \rightarrow pV; \quad V = \rho, \rho', \rho'', \omega, \phi, J/\Psi$$

and  $\gamma^*p \rightarrow X$  without introducing any new parameters.

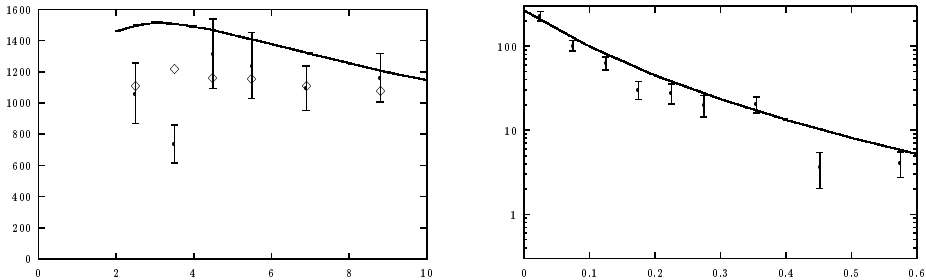


Fig. 10. Left: The scaled cross section  $Q^4 \sigma(Q^2)$  for  $\rho$ -production in nb.  $\text{GeV}^4$  as function of  $Q^2$  [ $\text{GeV}^2$ ]. The circles are the NMC-results and the diamonds represent our prediction [15] for the quantity  $Q^4 (\epsilon\sigma_L + \sigma_T)$  with the experimental polarization rate of NMC. Right: The differential cross section,  $d\sigma/dt(\Delta_T^2)$  [ $\text{nb GeV}^{-2}$ ] as function of  $t$  [ $\text{GeV}^2$ ], for  $\gamma^* + p \rightarrow \rho + p$  at  $Q^2 = 6 \text{ GeV}^2$ . Data from Ref. [40].

Generally the agreement with experiment is good, except for  $\phi$ -production where the model predictions are too large by a factor 2.

As an example I show in figure 10 the (parameter free) predictions for the  $Q^2$  and  $t$ -dependence of electroproduction of  $\rho^0$ -mesons.

#### 4.5. Soft and hard pomeron

As mentioned above the MSV as it stands predicts constant cross sections. In order to overcome this shortcoming an energy dependence in the spirit of the two pomerons of Donnachie and Landshoff [41] was introduced in the model in [32] in (roughly) the following way: If both dipoles are larger than the correlation length (ca. 0.35 fm) an energy dependence of a soft pomeron with intercept 1.08 is introduced, if one of the dipoles is smaller than that correlation length the energy dependence of a hard pomeron with intercept 1.28 is chosen. In that way a perfect fit to the proton structure function has been obtained over a huge range of  $W$  and  $Q^2$  values [32].

Of particular interest are  $\gamma^{(*)} - \gamma^{(*)}$  interactions, because in that case one can tune the size of both dipoles by varying the virtualities of the photons. The MSV has been applied to such reactions in [42, 43], in figure 11 the  $\gamma^{(*)} - \gamma^{(*)}$  cross section is given for real photons and photons with an average virtuality of  $14 \text{ GeV}^2$  as function of the CM energy  $W$ . Even for real photons the energy dependence is markedly stronger than for hadrons, a consequence of the concentration of the quarks at small distances due to the logarithmic singularity of the photon wave function (24). It can be seen from the figure 11 that for  $Q^2 = 14 \text{ GeV}^2$  the model grossly underestimates the contribution of the hard pomeron. The photon structure function is well predicted by the model [43].

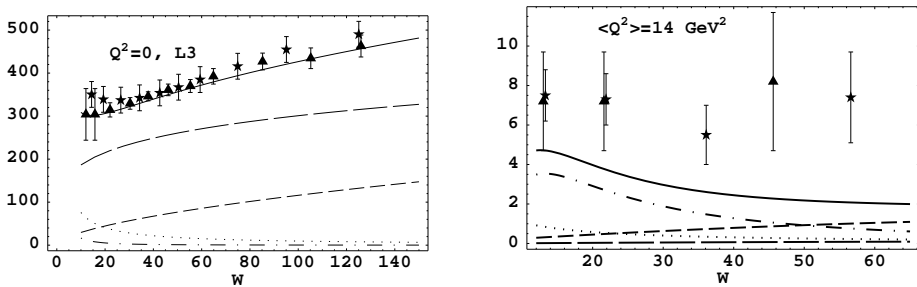


Fig. 11. Cross sections in nb for  $\gamma^{(*)}\gamma^{(*)}$  scattering for virtualities  $Q^2 = 0$  and  $14 \text{ GeV}^2$  respectively compared with L3 data. The solid curve is our model. It consists of the following contributions: soft pomeron: long dashes; hard pomeron: short dashes; fixed pole (box): dot-dashes; reggeon: dots; for details see reference [43].

4.6. The odderon problem

The odderon is the  $C, P$  partner of the pomeron (*i.e.* has an intercept near 1), but is odd under  $C$  and  $P$  transformations. It has been introduced in [44] and shown to be well compatible with axiomatic field theory. It contributes differently to  $pp$  and  $\bar{p}p$  scattering and can lead to a difference of the cross sections  $\sigma_{\bar{p}p} - \sigma_{pp}$  rising with energy  $W$ .

In QCD the odderon is by no means an odd concept since three or more gluons can couple to form a  $C = P = -1$  object. Therefore it must be present in perturbative QCD. This has renewed the interest in the odderon, especially in perturbative QCD (see [45, 46] and references there). In principle it is even more important in non-perturbative QCD since there is no small  $\alpha_s$  suppression!

The newer Tevatron data for  $p\bar{p}$  scattering and extrapolations of  $pp$ -scattering by DPR are compatible with

$$\Delta\rho = \frac{\text{Re}[T^{\bar{p}p}(t=0)]}{\text{Im}[T^{\bar{p}p}(t=0)]} - \frac{\text{Re}[T^{pp}(t=0)]}{\text{Im}[T^{pp}(t=0)]} \approx 0$$

which could not be the case if there is a sizeable odderon exchange.

A possible solution to this problem was proposed in [47]: If a quark-antiquark pair in the nucleon couples to a diquark with a size smaller than ca. 0.3 fm, the odderon coupling is strongly suppressed as can be seen from figure 12.

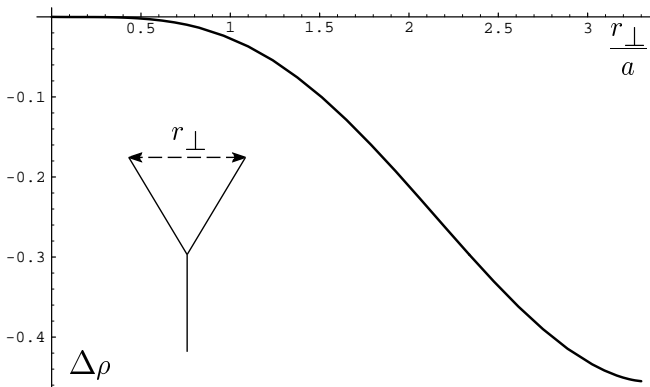


Fig. 12.  $\Delta\rho$  as a function of the “diquark size”  $r_{\perp}$  measured in units of the correlation length  $a \approx 0.35$  fm.

This suppression however does not take place if the proton breaks up [48]. Therefore a possible way to see the exchange of an odderon is to look for electroproduction of those mesons [46] which can only be produced by

$C = P = -1$  exchange and in which exchange the proton breaks up, *i.e.* processes like  $\gamma + p \rightarrow \pi_0 + X$  or  $\gamma + p \rightarrow f_2 + X$ . The cross section for the reaction  $\gamma + p \rightarrow \pi_0 + (2P)$  resp  $e + p \rightarrow e' + \pi_0 + (2P)$  is given in figure 13;  $2P$  stands for a quark diquark  $2P$ -state *i.e.*  $N^{(1/2,-)}$  or  $N^{(3/2,-)}$  [46].

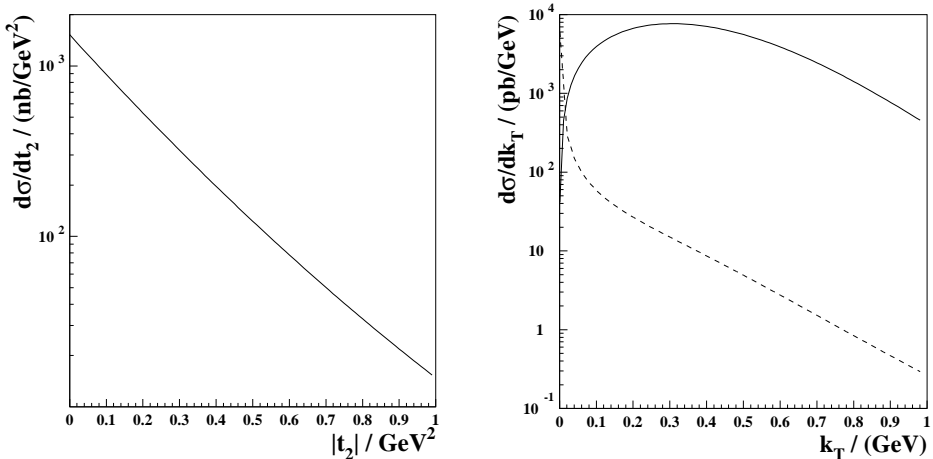


Fig. 13. Left: The differential cross section for the reaction  $\gamma + p \rightarrow \pi_0(2P)s$  as a function of the momentum transfer  $t$ . Right: The  $k_T$ -distribution in pion production for the reaction  $e + p \rightarrow e' + \pi_0 + (2P)$ : solid line: odderon contribution, dotted line: photon exchange; from [46].

It is a pleasure to thank the organizers of the conference for providing an at the same time stimulating and relaxed atmosphere

## REFERENCES

- [1] F.E. Low, *Phys. Rev.* **D12**, 163 (1975).
- [2] S. Nussinov, *Phys. Rev. Lett.* **34**, 1286 (1975).
- [3] P. Landshoff, O. Nachtmann, *Z. Phys.* **C35**, 405 (1987).
- [4] G. 't Hooft, in: *High Energy Physics*, A. Zichichi, editor, Bologna 1976.
- [5] S. Mandelstam, *Phys. Rep.* **23C**, 245 (1976).
- [6] B. Povh, J. Hüfner, *Phys. Rev. Lett.* **58**, 1612 (1987).
- [7] H.G. Dosch, *Phys. Lett.* **190B**, 177 (1987).
- [8] H.G. Dosch, Yu.A. Simonov, *Phys. Lett.* **205B**, 339 (1988).
- [9] H.G. Dosch, *Prog. Part. Nucl. Phys.* **33**, 121 (1994).

- [10] O. Nachtmann, 1996. hep-ph/9609365.
- [11] H.G. Dosch, In E. Ferreira *et al.*, editor, *Hadron Physics 96*, World Scientific, 1996.
- [12] O. Nachtmann, *Ann. Phys.* **209**, 436 (1991).
- [13] A. Kraemer, H.G. Dosch, *Phys. Lett.* **B272**, 114 (1991).
- [14] H.G. Dosch, E. Ferreira, A. Kramer, *Phys. Rev.* **D50**, 1992 (1994).
- [15] H.G. Dosch, T. Gousset, G. Kulzinger, H.J. Pirner, *Phys. Rev.* **D55**, 2602 (1997).
- [16] A.H. Mueller, Bimal Patel, *Nucl. Phys.* **B425**, 471 (1994).
- [17] A. Bialas, R. Peschanski, *Phys. Lett.* **B378**, 302 (1996).
- [18] Yu.A. Simonov, *Physics-Uspokhi* **39**, 0000 (1996).
- [19] H.G. Dosch, In A. Di Giacomo, D. Diakonov, editors, *Varenna-Lectures 1995*, Amsterdam 1996.
- [20] M.A. Shifman, A.I. Vainshtein, V.I. Zakharov, *Nucl. Phys.* **B147**, 385 (1979).
- [21] N.E. Balic, *Phys. Rev.* **D22**, 3090 (1980).
- [22] I.Ya. Aref'eva, *Teor. Mat. Fiz.* **43**, 111 (1980).
- [23] Yu.A. Simonov, *Yad. Fiz.* **48**, 1381 (1988).
- [24] A. Di Giacomo, H. Panagopoulos, *Phys. Lett.* **B285**, 133 (1992).
- [25] Massimo D'Elia, A. Di Giacomo, E. Meggiolaro, *Phys. Lett.* **B408**, 315 (1997).
- [26] M. Schiestl, H.G. Dosch, *Phys. Lett.* **209B**, 85 (1988).
- [27] Yu.A. Simonov, *Nucl. Phys.* **B324**, 67 (1989).
- [28] N. Brambilla, A. Vairo, *Phys. Rev.* **D55**, 3974 (1997).
- [29] M. Rueter, H.G. Dosch, *Z. Phys.* **C66**, 245 (1995).
- [30] G.S. Bali, K. Schilling, C. Schlichter, *Phys. Rev.* **D51**, 5165 (1995).
- [31] H.G. Dosch, T. Gousset, H.J. Pirner, *Phys. Rev.* **D57**, 1666 (1998).
- [32] Michael Rueter, *Eur. Phys. J.* **C7**, 233 (1999).
- [33] E.R. Berger, O. Nachtmann, *Eur. Phys. J.* **C7**, 459 (1999).
- [34] Enrico Meggiolaro, *Phys. Lett.* **B451**, 414 (1999).
- [35] V.A. Novikov, M.A. Shifman, A.J. Vainshtein, V.I. Zakharov, *Nucl. Phys.* **B191**, 301 (1981).
- [36] J. Nemchik, N.N. Nikolaev, E. Predazzi, B.G. Zakharov, *Phys. Lett.* **B374**, 199 (1996). see also hep-ph-9605231.
- [37] M. Rueter, H.G. Dosch, *Phys. Rev.* **D57**, 4097 (1998).
- [38] H.G. Dosch, F.S. Navarra, M. Nielsen, M. Rueter, 1999.
- [39] G. Kulzinger, H.G. Dosch, H.J. Pirner, *Eur. Phys. J.* **C7**, 73 (1999).
- [40] M. Arneodo *et al.*, *Nucl. Phys.* **B429**, 503 (1994).
- [41] A. Donnachie, P.V. Landshoff, *Phys. Lett.* **B437**, 408 (1998).
- [42] A. Donnachie, H.G. Dosch, M. Rueter, *Phys. Rev.* **D59**, 074011 (1999).
- [43] A. Donnachie, H.G. Dosch, M. Rueter, 1999, hep-ph/9908413.

- [44] L. Lukazuk, B. Nicolescu, *Nuovo Cim. Lett.* **8**, 405 (1973).
- [45] B. Nicolescu, 1998, hep-ph/9810465 and references therein.
- [46] E.R. Berger *et al.* *Eur. Phys. J.* **C9**, 491 (1999).
- [47] M. Rueter, H.G. Dosch, *Phys. Lett.* **B380**, 177 (1996).
- [48] M. Rueter, H.G. Dosch, O. Nachtmann, *Phys. Rev.* **D59**, 014018 (1999).